AD
Reports Control Symbol
OSD-1366

ADA040841

RESEARCH AND DEVELOPMENT TECHNICAL REPORT
ECOM-5597

RESPONSE CALCULATIONS FOR A COMMERCIAL LIGHT - SCATTERING AEROSOL COUNTER

By

R. G. Pinnick
E. B. Stenmark

Atmospheric Sciences Laboratory
US Army Electronics Command
White Sands Missile Range, New Mexico 88002

July 1976

DDC
RECEIVED
JUN 23 1977
C

Approved for public release; distribution unlimited.

AD No. ____
DDC FILE COPY

ECOM

UNITED STATES ARMY ELECTRONICS COMMAND - FORT MONMOUTH, NEW JERSEY 07703

NOTICES

Disclaimers

The findings in this report are not to be construed as an official Department of the Army position, unless so designated by other authorized documents.

The citation of trade names and names of manufacturers in this report is not to be construed as official Government indorsement or approval of commercial products or services referenced herein.

Disposition

Destroy this report when it is no longer needed. Do not return it to the originator.

SECURITY CLASSIFICATION OF THIS PAGE *(When Data Entered)*

REPORT DOCUMENTATION PAGE

READ INSTRUCTIONS BEFORE COMPLETING FORM

1. REPORT NUMBER: ECOM-5597	2. GOVT ACCESSION NO.
3. RECIPIENT'S CATALOG NUMBER	
4. TITLE (and Subtitle): RESPONSE CALCULATIONS FOR A COMMERCIAL LIGHT-SCATTERING AEROSOL COUNTER	5. TYPE OF REPORT & PERIOD COVERED
	6. PERFORMING ORG. REPORT NUMBER
7. AUTHOR(s): R. G. Pinnick E. B. Stenmark	8. CONTRACT OR GRANT NUMBER(s)
9. PERFORMING ORGANIZATION NAME AND ADDRESS: Atmospheric Sciences Laboratory White Sands Missile Range, New Mexico 88002	10. PROGRAM ELEMENT, PROJECT, TASK AREA & WORK UNIT NUMBERS: DA Task 1T511103
11. CONTROLLING OFFICE NAME AND ADDRESS: US Army Electronics Command Fort Monmouth, New Jersey 07703	12. REPORT DATE: July 1976 13. NUMBER OF PAGES: 31
14. MONITORING AGENCY NAME & ADDRESS *(if different from Controlling Office)*	15. SECURITY CLASS. *(of this report)*: UNCLASSIFIED 15a. DECLASSIFICATION/DOWNGRADING SCHEDULE

16. DISTRIBUTION STATEMENT *(of this Report)*

Approved for public release; distribution unlimited.

17. DISTRIBUTION STATEMENT *(of the abstract entered in Block 20, if different from Report)*

18. SUPPLEMENTARY NOTES

19. KEY WORDS *(Continue on reverse side if necessary and identify by block number)*

Aerosol counter
Particle size distribution
Aerosol measurement

20. ABSTRACT *(Continue on reverse side if necessary and identify by block number)*

To adequately assess the effect of atmospheric aerosols on electro-optical and high energy laser systems, particulate size distributions must be measured. Single particle light scattering aerosol particle counters offer some advantages for these measurements. This report presents response calculations for a commercially available light-scattering aerosol particle counter (the Particle Measurement Systems Classical Scattering Aerosol Spectrometer) used by the DoD community for such measurements. The calculations are for spherical particles → next page

DD FORM 1 JAN 73 1473 EDITION OF 1 NOV 65 IS OBSOLETE

SECURITY CLASSIFICATION OF THIS PAGE *(When Data Entered)*

037620

20. Abstract (cont)

cont →

and consider the wavelength of the laser source and the geometry of the light-collecting optics. The results show a strong dependence of the response upon the particle refractive index and multivalued response for particles with diameter greater than 0.8 micrometer. The problem of deconvolution of size distribution information from measurements taken with this instrument is addressed. Several examples of size distribution measurements of atmospheric fog and haze are given to illustrate the significance of the results.

SUMMARY

Mie theory response calculations presented for the Particle Measurement Systems Classical Scattering Aerosol Spectrometer show the particle size resolution for spherical particles of unknown composition to be less than advertised for aerosols with refractive indexes in the range of those of atmospheric aerosols. However, for spherical particles of known composition, these results can be used to group and redefine the particle size channels to avoid regions of multivalued response and thereby optimize the size resolution of the instrument. For particles of mixed composition, only a small number of size channels are justified. Field measurements on atmospheric fog and haze suggest that the response calculations apply to the instrument, although controlled laboratory measurements on uniform aerosols of known composition and size are required for a definitive confirmation of the theoretical response calculations shown here.

CONTENTS

INTRODUCTION

Light scattering aerosol particle counters are used for determination of size distribution and concentration of aerosol particles. These devices work on the principle that as aerosol particles flow through an illuminated volume, light scattered into a particular solid angle by a single particle is measured photoelectrically and is used to determine particle size by electronically classifying response pulses according to their magnitude. Determination of particle size from the response is difficult because of the complicated dependence of the response on particle size, particle index of refraction, the lens geometry of the counter optical system, and for instruments with broadband sources - the phototube spectral sensitivity. These difficulties have been studied previously [1-4] for several aerosol counters including the commercially available Climet, Bausch and Lomb 40-1A, Royco 245, Royco 220, Royco 218, and the Jacobi.

The purpose of this report is to present new light-scattering calculations for the response of an instrument that has recently become commercially available: the Particle Measurement Systems, Inc., Classical Scattering Aerosol Spectrometer (CSAS).

COUNTER RESPONSE CALCULATION

The theoretical response of the CSAS to a particle of a particular size and refractive index can be expressed as a cross section per particle for light scattered into the particular solid angle of the instrument collecting optics. This response is given by

$$\int_{\theta=4^\circ}^{\theta=22^\circ} \frac{\lambda^2}{4\pi} [i_1(m, x, \theta) + i_2(m, x, \theta)] \sin\theta \, d\theta$$

where λ is the wavelength of the light and $i_1(m, x, \theta)$ and $i_2(m, x, \theta)$ are the angular intensity functions. The above expression integrated over all thetas yields the total scattering cross section. The angular intensity functions depend on m, the complex refractive index of the particle; the particle size parameter x defined as the ratio of the particle circumference to the wavelength; and the scattering angle θ as measured from the direction of forward scattering. The light-collecting solid angle for the CSAS instrument has axial symmetry and is for values of theta from 4° through 22° from the direction of forward scattering. The wavelength is that for a He-Ne laser, 6328Å.

It is well known that at a particular scattering angle the scattered intensity is an oscillatory function of size parameter so that a single

measurement may not yield a single value of particle size. However, the hope is that averaging of these intensity functions over a considerable range of scattering angles will damp out the oscillations to give a single-valued response curve. It is desirable that the response curves be nearly the same for materials of different refractive index, since in practice the particle composition may not be known.

Response calculations for the CSAS instrument for water particles with refractive index 1.33-0i, for ammonium sulfate particles with index 1.5-0i, and for absorbing atmospheric dust particles with indexes 1.50-0.01i and 1.5-0.05i are shown in Figure 1. The results show a strong dependence of the response upon the particle refractive index and multivalued response for particles with diameter greater than about 0.8 micrometer. The calculated response is obviously sensitive to the particle refractive index for indexes in the range of those of atmospheric aerosols. The seriousness of the multivaluedness is reduced if only a small number of particle size channels are utilized in the multichannel analyzer. Of course, the size resolution of the instrument is reduced accordingly. Based upon these calculations for the range of particulate refractive indexes considered here, the instrument size resolution is 0.9 to 1.6 microns for particles of 1-micron diameter, 3 to 9 microns for particles of 4-micron diameter, and 7 to 17 microns for particles of 10-micron diameter. For comparison, the advertised resolution is ±10% for particles less than 20-micron diameter and ±2 microns for particles larger than 20-micron diameter.

The manufacturer's calibration for our particular CSAS instrument is given in the table. The corresponding discriminator level settings are indicated by tick marks in Figure 1. There are 15 particle size channels for each "range" of the instrument. Pulse height channels 1, 5, 10, and 15 are labeled between the appropriate tick marks. Changing range is merely an adjustment of an amplifier gain and so has the effect of shifting the range of sensitivity.

Even if the particulates measured are all of the same known composition, there are - on some ranges - discriminator levels set in regions of multivalued response. Nevertheless, size distribution information for such a polydispersion of spherical particles can be determined by reducing the number of channels to avoid these regions. The effects of such a grouping of the particle size channels on the inferred particle size distribution for measurements of atmospheric fog and haze under the assumption that the particles are water droplets are presented in the next section.

SIZE DISTRIBUTION MEASUREMENTS OF ATMOSPHERIC FOG AND HAZE WITH THE CSAS

If spherical particles of known composition are measured with the CSAS, size distribution information may be obtained from the theoretical results

PARTICLE SIZE CHANNEL WIDTHS (Diameter in μm)

FOR THE CSAS-100,

AS SPECIFIED BY THE MANUFACTURER

	Instrument Range			
Channel	1	2	3	4
1	2-4	1-2	0.5-1	0.4-0.65
2	4-6	2-3	1-1.5	0.65-0.9
3	6-8	3-4	1.5-2.0	0.9-1.15
4	8-10	4-5	2.0-2.5	1.15-1.4
5	10-12	5-6	2.5-3.0	1.4-1.65
6	12-14	6-7	3.0-3.5	1.65-1.9
7	14-16	7-8	3.5-4.0	1.9-2.15
8	16-18	8-9	4.0-4.5	2.15-2.4
9	18-20	9-10	4.5-5.0	2.4-2.65
10	20-22	10-11	5.0-5.5	2.65-2.9
11	22-24	11-12	5.5-6.0	2.9-3.2
12	24-26	12-13	6.0-6.5	3.2-3.5
13	26-28	13-14	6.5-7.0	3.5-3.8
14	28-30	14-15	7.0-7.5	3.8-4.1
15	30-32	15-16	7.5-8.0	4.1-4.4

presented here by grouping the particle size channels to avoid problems of multivalued response. This channel redefinition for water particles is shown along with the response curve in Figure 2. The heavy tick marks indicate the redefined channels. The light and heavy tick marks together indicate the advertised channel discriminator levels and are identical to those in Figure 1. The channels are redefined with less size resolution than the response curve dictates because in practice statistical spectra broadening effects result in some channel cross sensitivity. Specifically, even a perfectly monodisperse aerosol results in a range of pulse heights, and identical particles are not counted entirely in one particle size channel. Therefore, setting discriminator levels near regions of multivalued response has been avoided. The recalibration reduces the number of channels for each range from 15 to 7. The redefined channels are not of equal width.

The effect of this recalibration on size distributions of atmospheric fog and haze inferred from measurements with the CSAS is shown in Figures 3 through 13. These particulate size distributions are shown to corroborate our recalibration. According to the response calculation, the manufacturer-advertised calibration may lead to artificial maxima in the inferred size distribution in regions of multivalued response and relative minima between these regions. In regions of multivalued response, particles with a relatively large range of sizes produce response pulses in a small range of pulse heights; whereas, between regions of multivalued response, particles with a relatively narrow range of sizes produce response pulses in a comparable range of pulse heights. Therefore, if the manufacturer's calibration is used, distortion of the real size distribution of a polydispersion of fog or haze to be inferred from measurements with this instrument would be expected. Such artifacts in the distributions would be most noticeable in the form of relative maxima in regions of multivalued response (i.e., at 0.6-1.3, 1.6-2.2 micron radii) and relative minima between these regions (i.e., at about 1.5 micron radius). These distortions could be seen easily only if the pulse height discriminators are set with sufficient resolution.

Examination of the manufacturer calibration-derived size distributions in Figures 3 through 9 show evidence of these artifacts. However, they are not evident in Range 1 data in Figures 10 and 11 since the pulse height discriminators on this setting of the instrument are not set sufficiently close to resolve them. The fact that these relative maxima and minima occur for a variety of very different size distributions suggests that they are artifacts resulting from the Mie resonances in our calculation of the instrument response, since they are not evident in the size distributions determined from the recalibration. It is noteworthy that the overall form of size distribution inferred from the manufacturer calibration and from our redefined calibration is in agreement. Such would not be the case for absorptive particles.

This recalibration scheme has also been applied to a similar model of the CSAS owned by the Night Vision Laboratory which is identical to the instrument studied here except that the pulse height discriminator levels are set differently. Some results of the recalibration on size distribution measurements on atmospheric fog are shown in Figures 12 and 13. The smooth curves are those obtained with the manufacturer calibration and the dashed curves with our recalibration scheme. Measurements made on the four range settings are plotted on one figure since they were made sequentially during relatively stable fog conditions. It is suggested that the plateaus in the manufacturer calibration-inferred size distribution at approximately 1 and 2 micron radius are a result of the multivaluedness in the response curve in Figure 2.

The effect of this recalibration on particulate extinction cross sections calculated from the size distribution data for 1, 4, and 10 micron radiation depends on the size distribution and on the particular range that the instruments are set on. For a variety of fog and haze measurements, however, the extinction calculated via the redefined calibration versus the manufacturer calibration generally differs by a factor of 50% or less at 1 micron and by a factor of 2 or less at 4 and 10 microns.

The manufacturer has made two comments bearing on the results presented here. One is that the classical scattering instrument (CSAS) is not always produced with the degree of pulse height resolution capable of the particular models studied here. For these instruments the multivalued response problem may be less important, depending on where the discriminator levels are set. Secondly, the manufacturer says that since the lasers in the instruments operate in multimode, the phase shifts through the beam cause smoothing of the resonances in the response curves, as the scattering process is no longer described exactly by Mie theory. The authors do not think this second comment has validity, although controlled laboratory measurements on uniform aerosols of known composition and size are required for a definitive confirmation of the Mie theory response calculations shown here.

REFERENCES

1. Cooke, Derry D. and Milton Kerker, March 1975, "Response Calculations for Light-Scattering Aerosol Particle Counters," Appl. Opt., Vol 14, No. 3, pp 734-739.

2. Quenzel, H., January 1969, "Influence of Refractive Index on the Accuracy of Size Determination of Aerosol Particles with Light-Scattering Aerosol Counters," Appl. Opt., Vol 8, No. 1, pp 165-169.

3. Pinnick, R. G., J. M. Rosen, and D. J. Hofmann, January 1973, "Measured Light-Scattering Properties of Individual Aerosol Particles Compared to Mie Scattering Theory," Appl. Opt., Vol 12, No. 1, pp 37-41.

4. Hodkinson, J. Raymond and Judith R. Greenfield, November 1965, "Response Calculations for Light-Scattering Aerosol Counters and Photometers," Appl. Opt., Vol 4, No. 11, pp 1463-1474.

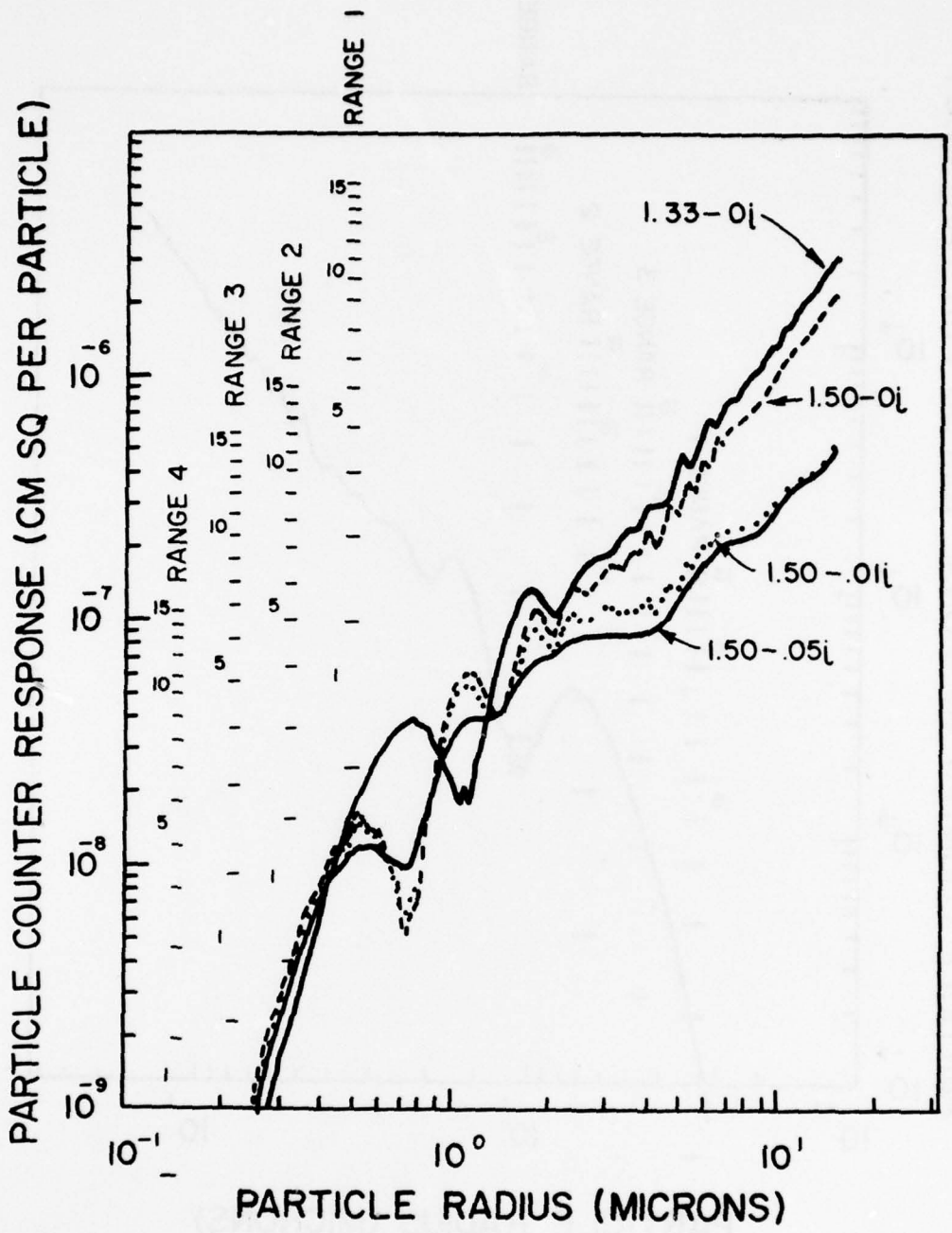

Figure 1. Response calculations for the Particle Measurement Systems CSAS instrument for water particles with refractive index 1.33-0i, ammonium sulfate particles with refractive index 1.50-0i, and absorbing atmospheric dust with indexes 1.50-0.01i and 1.50-0.05i. The tick marks indicate the pulse height discriminator level settings for the instrument. Channels 1, 5, and 15 are labeled between the appropriate tick marks for the different range settings of the instrument.

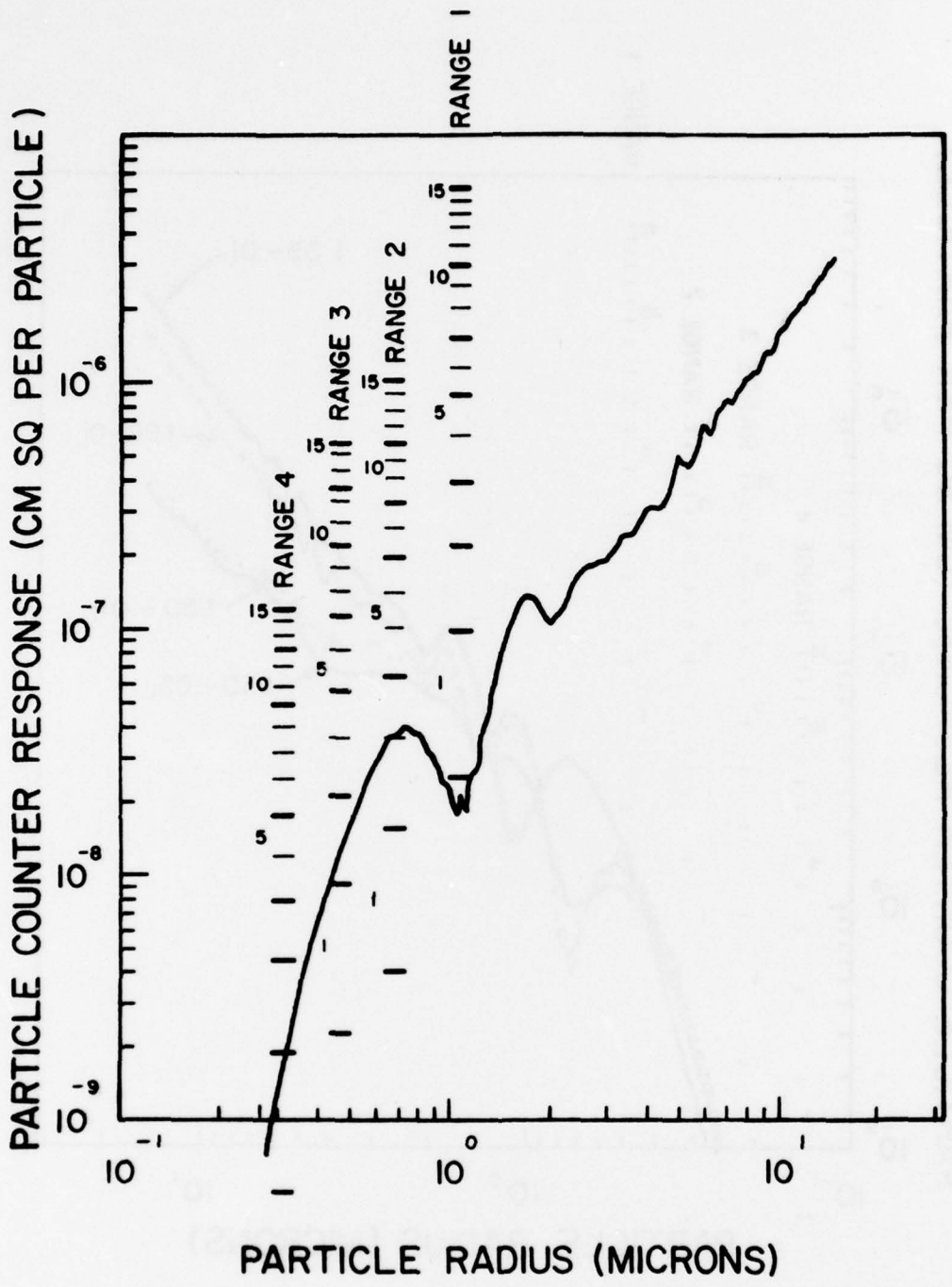

Figure 2. Response calculations for the Particle Measurement Systems CSAS instrument for water particles. The heavy tick marks indicate - for the different instrument ranges - the pulse height discriminator level settings used in grouping channels to avoid regions of multivalued response. The light and heavy tick marks together indicate the manufacturer discriminator level settings and are identical to those in Figure 1. Channels 1, 5, and 15 are labeled between the appropriate tick marks.

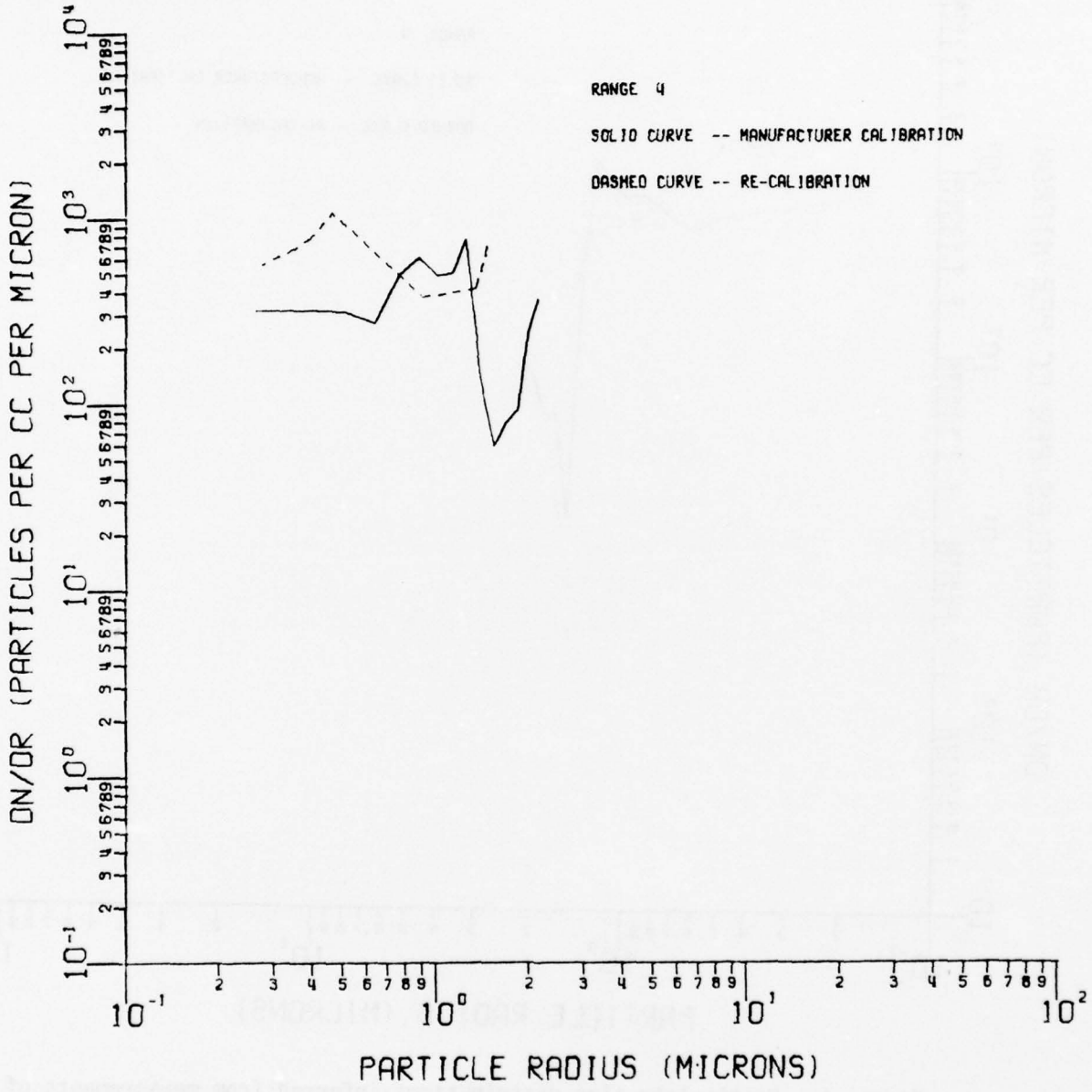

Figure 3. Particulate size distributions inferred from measurements of atmospheric fog made with the CSAS using the manufacturer calibration (solid curve) and the Mie theory recalibration (dashed curve).

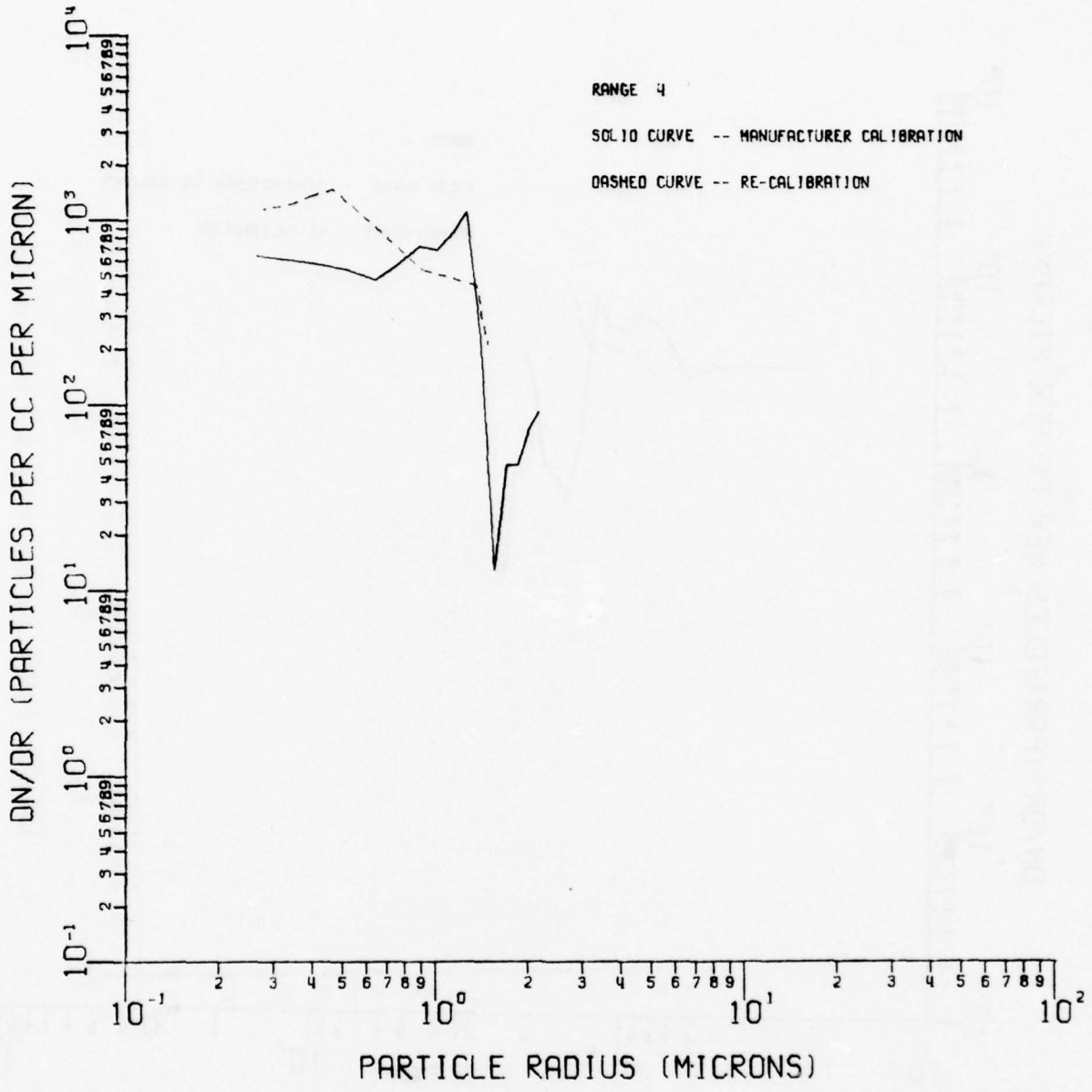

Figure 4. Particulate size distributions inferred from measurements of atmospheric fog made with the CSAS using the manufacturer calibration (solid curve) and the Mie theory recalibration (dashed curve).

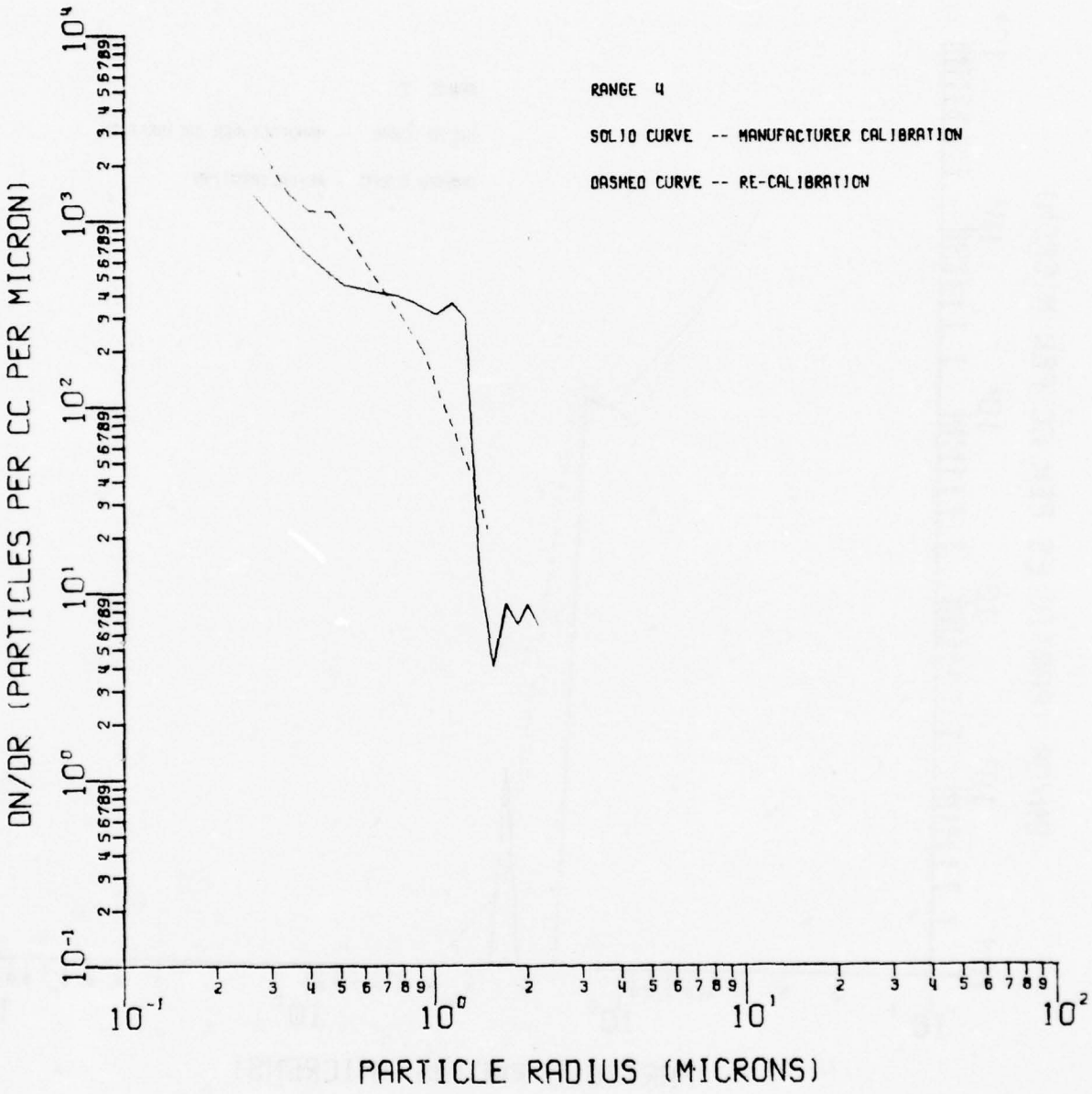

Figure 5. Particulate size distributions inferred from measurements of atmospheric haze made with the CSAS using the manufacturer calibration (solid curve) and the Mie theory recalibration (dashed curve).

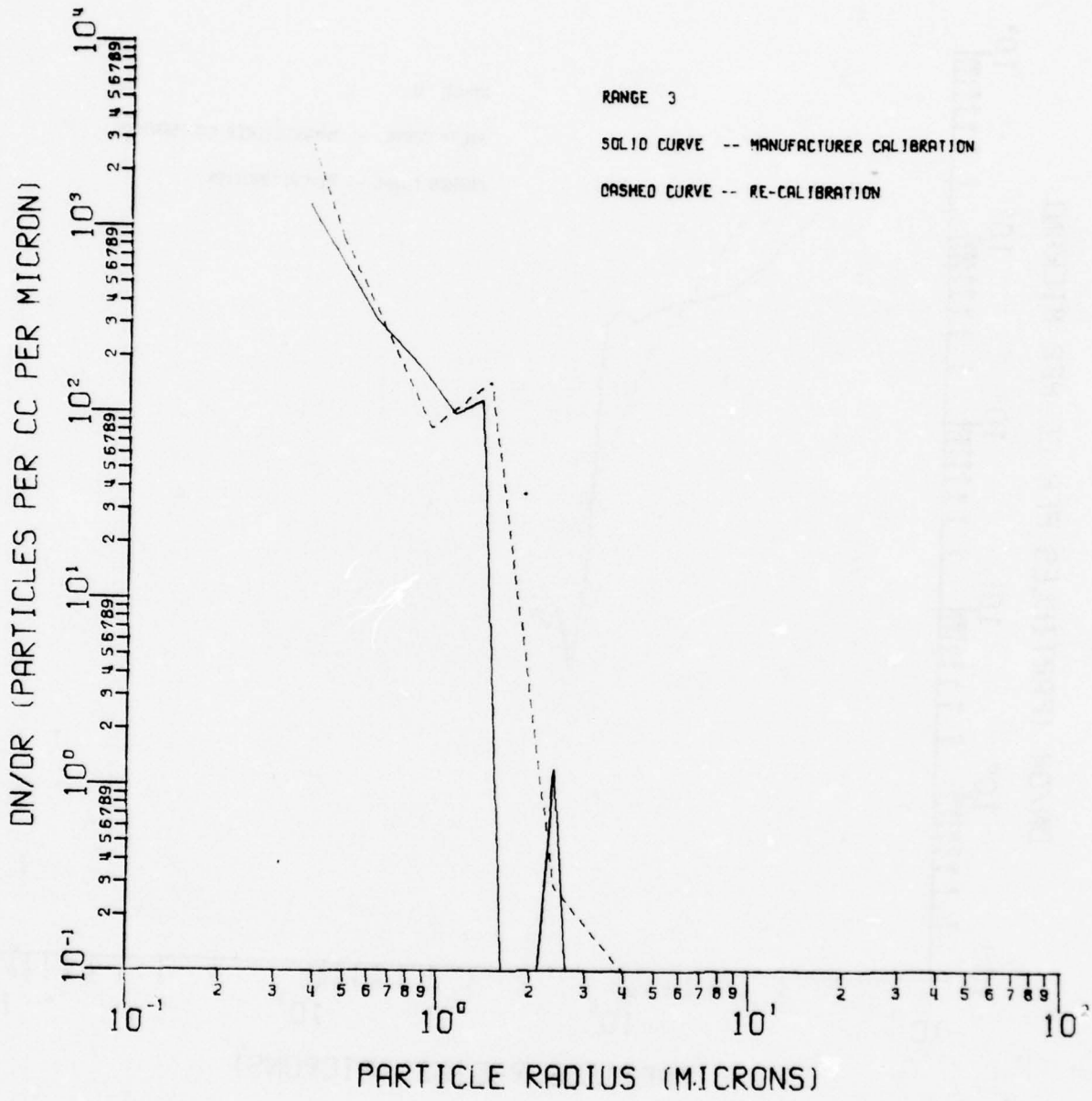

Figure 6. Particulate size distributions inferred from measurements of atmospheric haze made with the CSAS using the manufacturer calibration (solid curve) and the Mie theory recalibration (dashed curve).

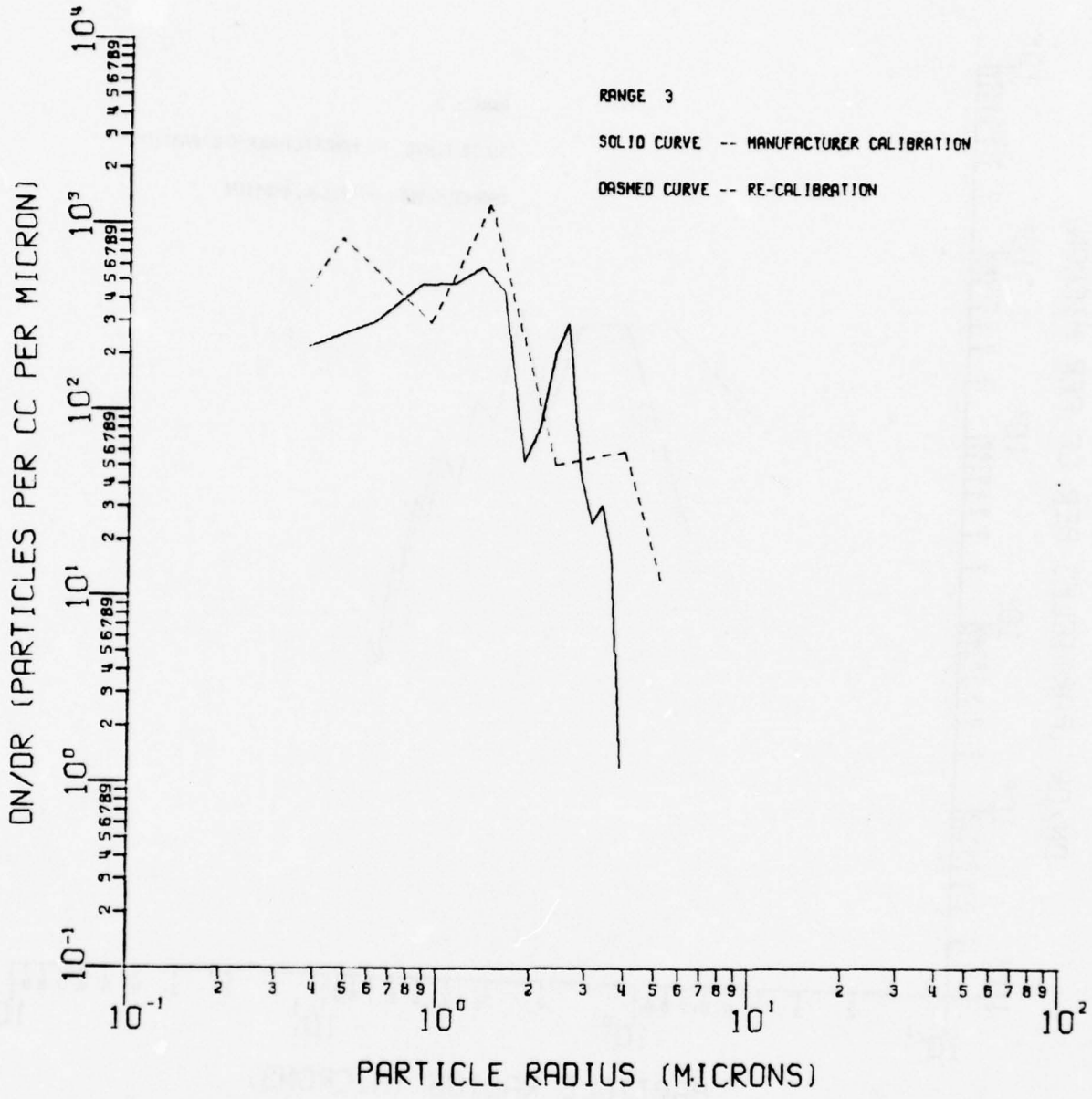

Figure 7. Particulate size distributions inferred from measurements of atmospheric haze made with the CSAS using the manufacturer calibration (solid curve) and the Mie theory recalibration (dashed curve).

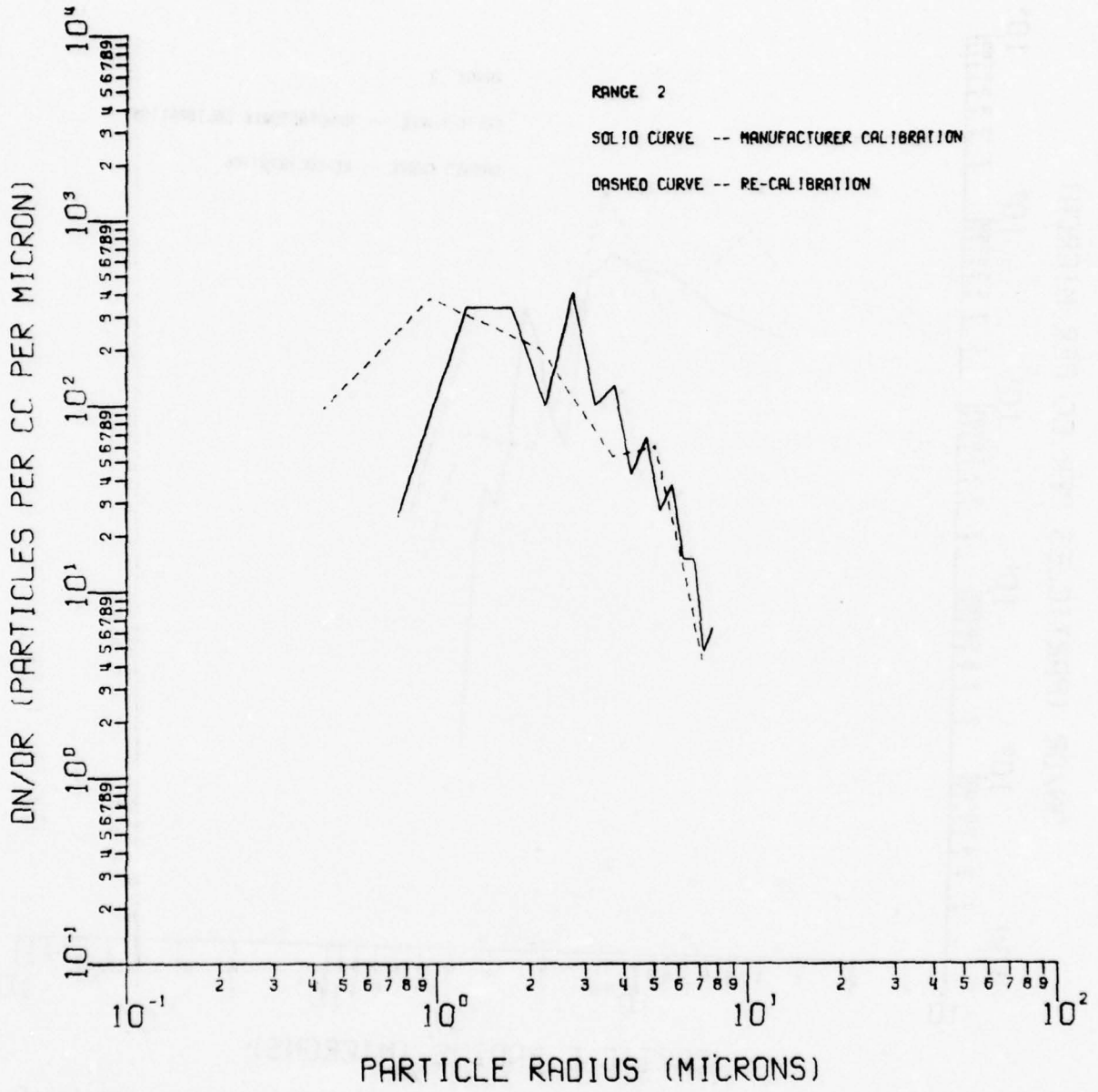

Figure 8. Particulate size distributions inferred from measurements of atmospheric fog made with the CSAS using the manufacturer calibration (solid curve) and the Mie theory recalibration (dashed curve).

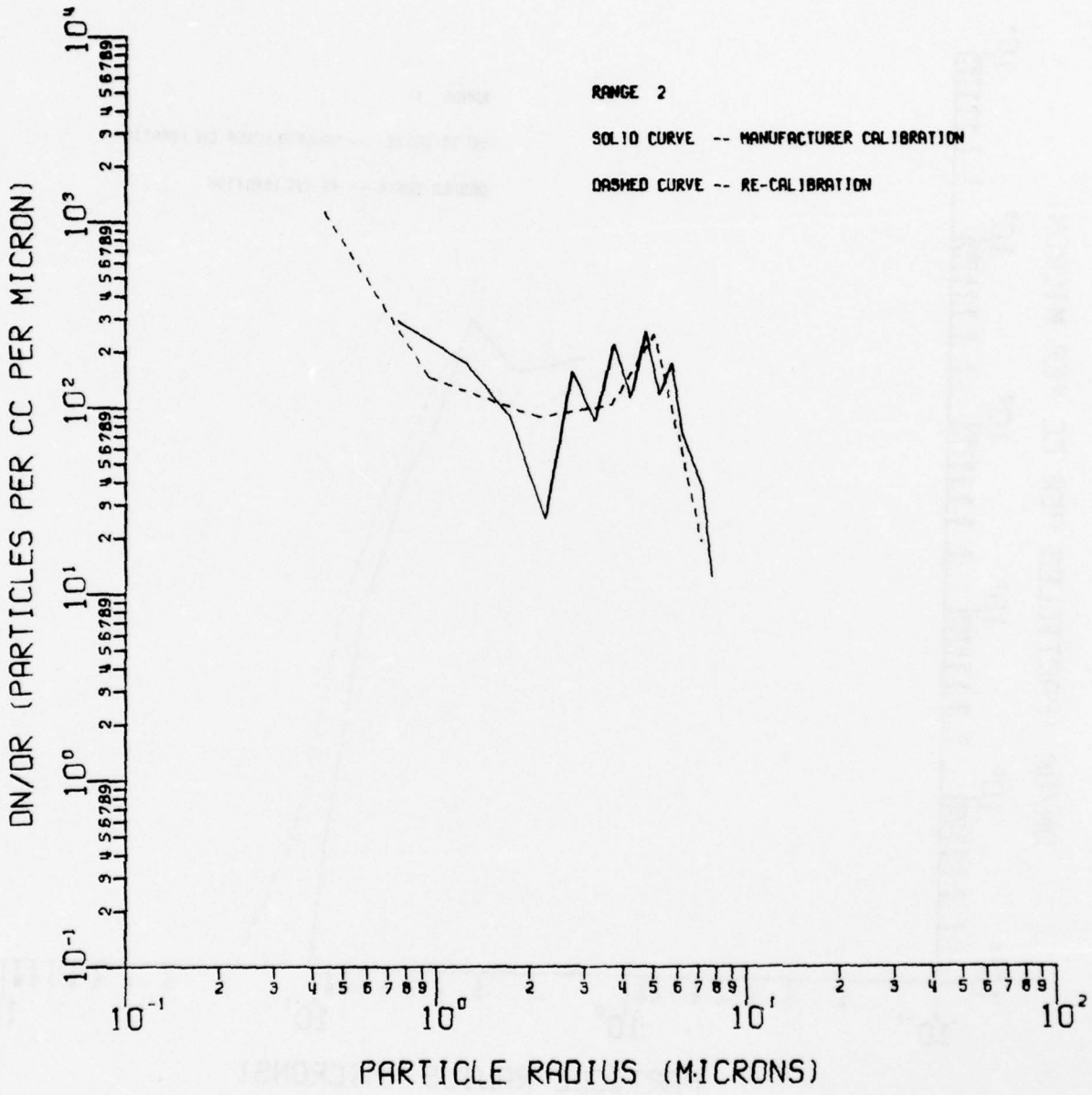

Figure 9. Particulate size distributions inferred from measurements of atmospheric fog made with the CSAS using the manufacturer calibration (solid curve) and the Mie theory recalibration (dashed curve).

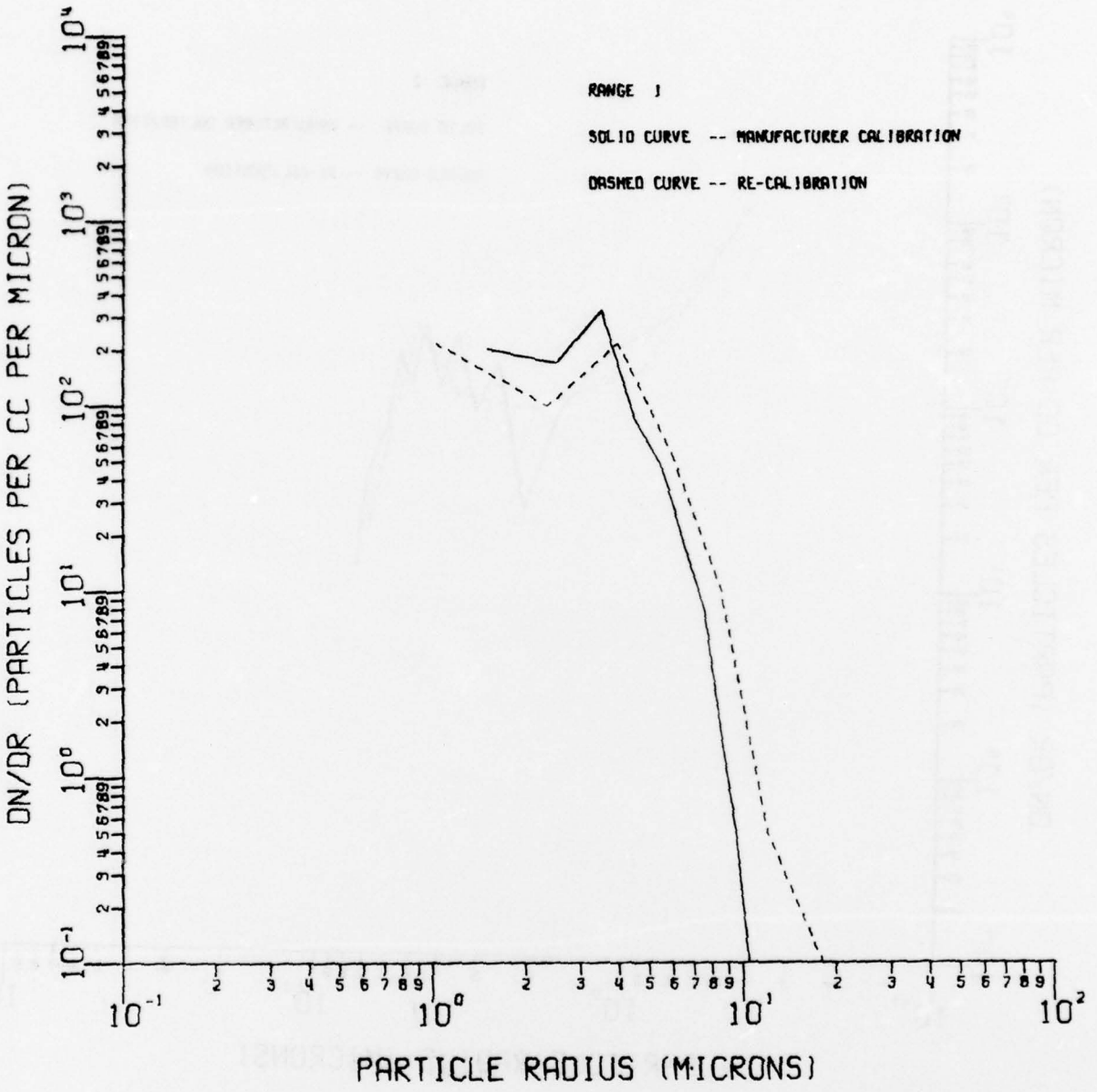

Figure 10. Particulate size distributions inferred from measurements of atmospheric fog made with the CSAS using the manufacturer calibration (solid curve) and the Mie theory recalibration (dashed curve).

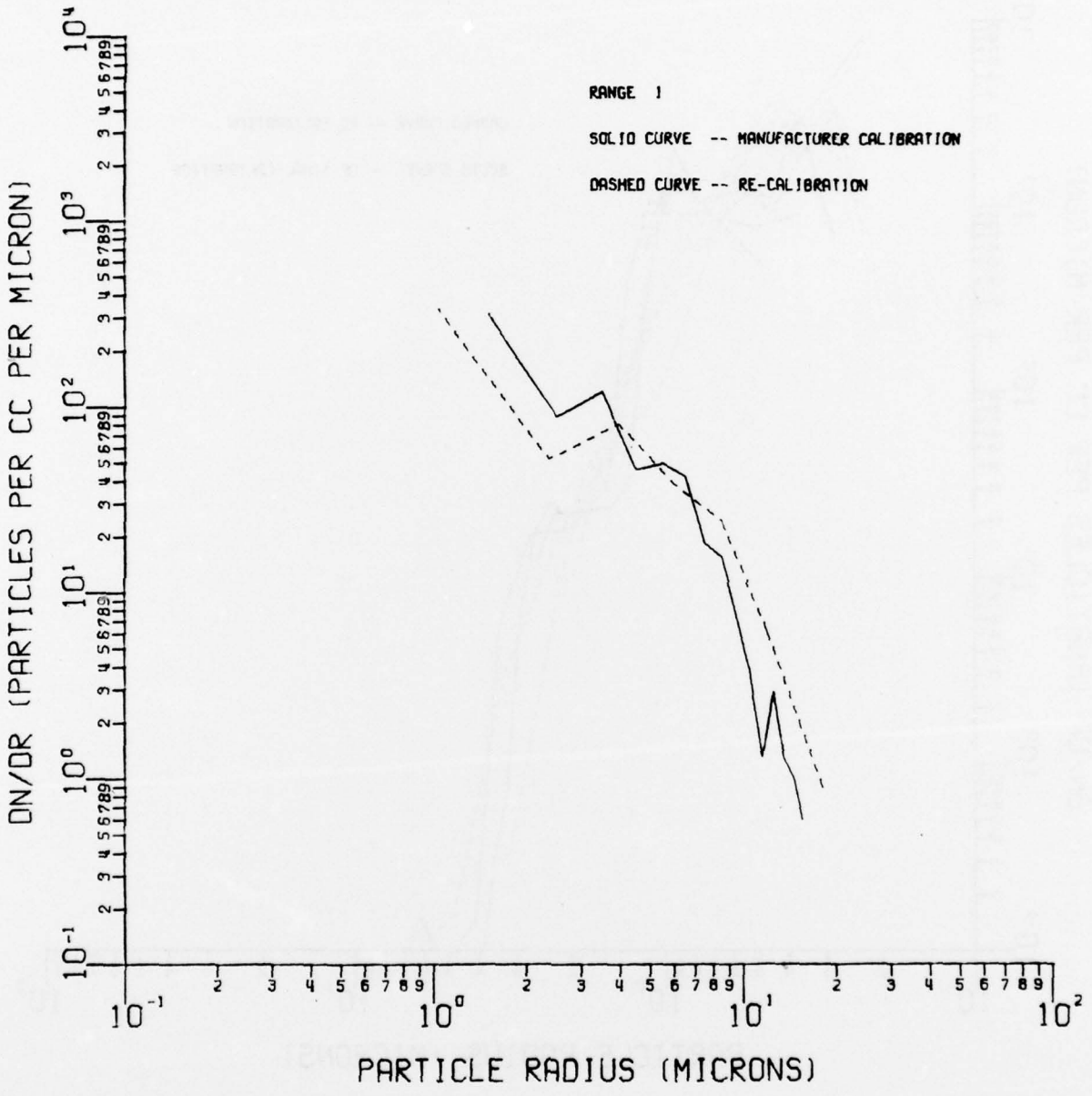

Figure 11. Particulate size distributions inferred from measurements of atmospheric fog made with the CSAS using the manufacturer calibration (solid curve) and the Mie theory recalibration (dashed curve).

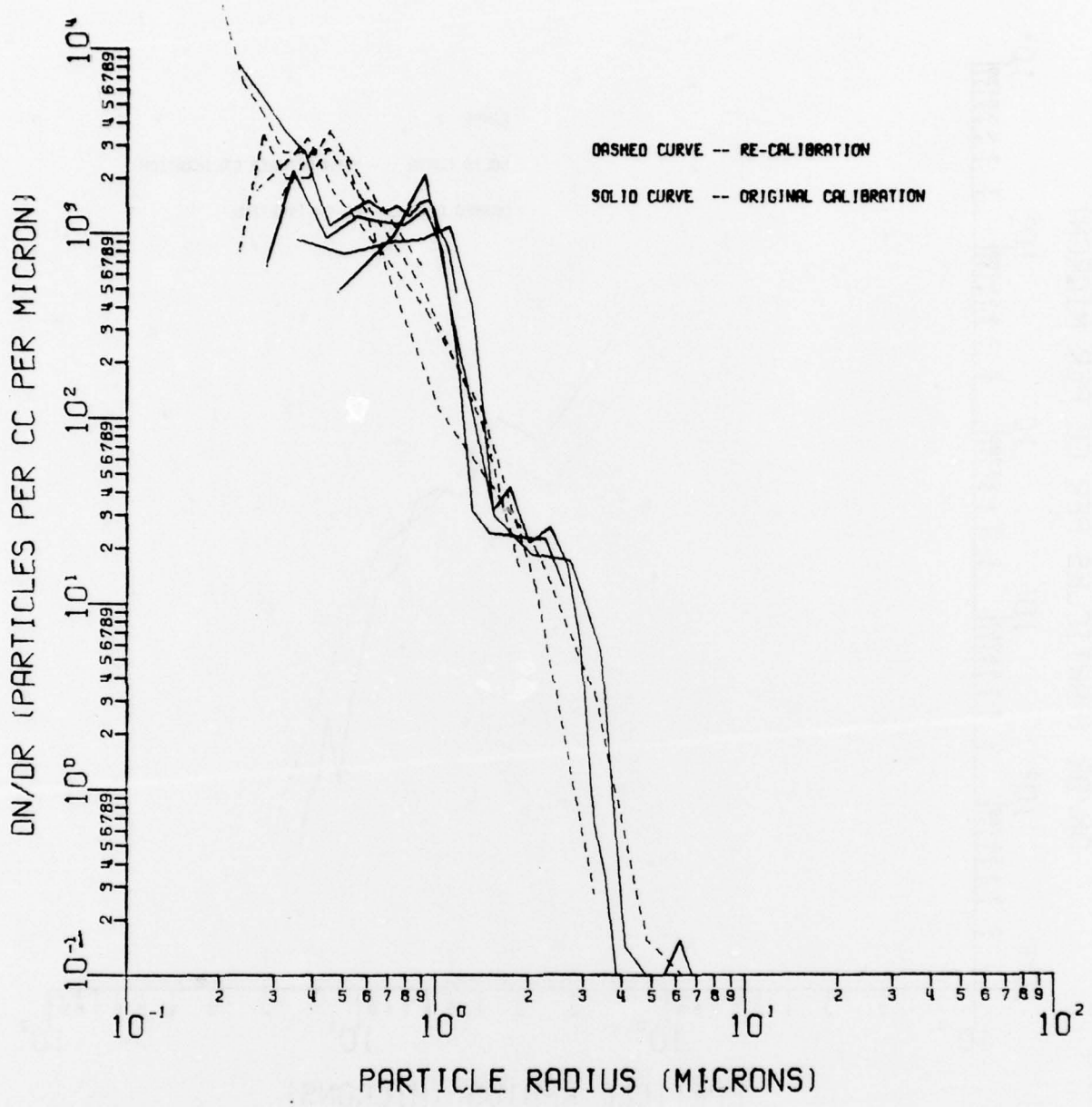

Figure 12. Particulate size distributions inferred from measurements of atmospheric fog made with the CSAS using the manufacturer calibration (solid curve) and the Mie theory recalibration (dashed curve).

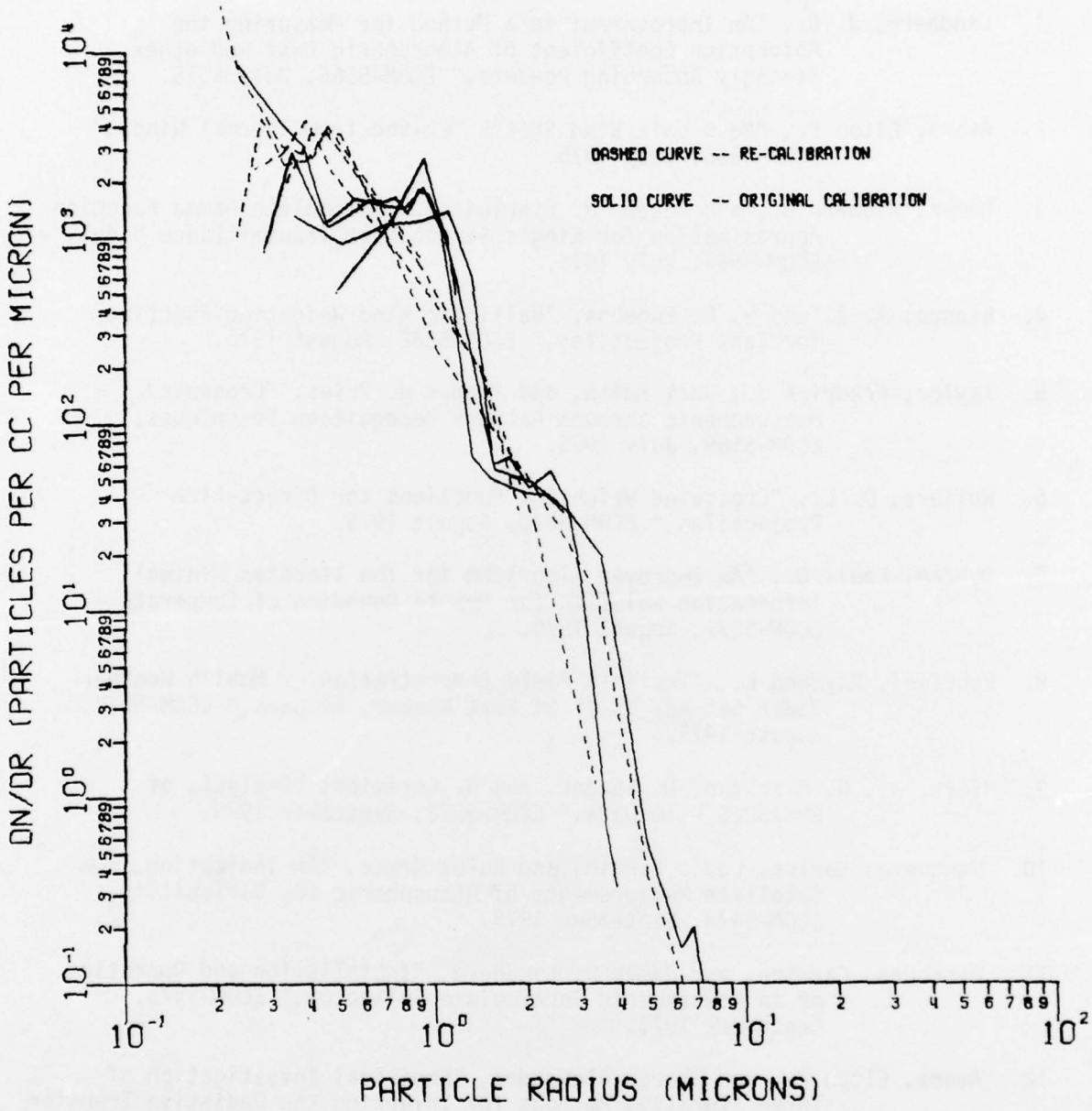

Figure 13. Particulate size distributions inferred from measurements of atmospheric fog made with the CSAS using the manufacturer calibration (solid curve) and the Mie theory recalibration (dashed curve).

ATMOSPHERIC SCIENCES RESEARCH PAPERS

1. Lindberg, J. D., "An Improvement to a Method for Measuring the Absorption Coefficient of Atmospheric Dust and other Strongly Absorbing Powders," ECOM-5565, July 1975.

2. Avara, Elton P., "Mesoscale Wind Shears Derived from Thermal Winds," ECOM-5566, July 1975.

3. Gomez, Richard B., and Joseph H. Pierluissi, "Incomplete Gamma Function Approximation for King's Strong-Line Transmittance Model," ECOM-5567, July 1975.

4. Blanco, A. J. and B. F. Engebos, "Ballistic Wind Weighting Functions for Tank Projectiles," ECOM-5568, August 1975.

5. Taylor, Fredrick J., Jack Smith, and Thomas H. Pries, "Crosswind Measurements through Pattern Recognition Techniques," ECOM-5569, July 1975.

6. Walters, D. L., "Crosswind Weighting Functions for Direct-Fire Projectiles," ECOM-5570, August 1975.

7. Duncan, Louis D., "An Improved Algorithm for the Iterated Minimal Information Solution for Remote Sounding of Temperature," ECOM-5571, August 1975.

8. Robbiani, Raymond L., "Tactical Field Demonstration of Mobile Weather Radar Set AN/TPS-41 at Fort Rucker, Alabama," ECOM-5572, August 1975.

9. Miers, B., G. Blackman, D. Langer, and N. Lorimier, "Analysis of SMS/GOES Film Data," ECOM-5573, September 1975.

10. Manquero, Carlos, Louis Duncan, and Rufus Bruce, "An Indication from Satellite Measurements of Atmospheric CO_2 Variability," ECOM-5574, September 1975.

11. Petracca, Carmine, and James D. Lindberg, "Installation and Operation of an Atmospheric Particulate Collector," ECOM-5575, September 1975.

12. Avara, Elton P., and George Alexander, "Empirical Investigation of Three Iterative Methods for Inverting the Radiative Transfer Equation," ECOM-5576, October 1975.

13. Alexander, George D., "A Digital Data Acquisition Interface for the SMS Direct Readout Ground Station - Concept and Preliminary Design," ECOM-5577, October 1975.

14. Cantor, Israel, "Enhancement of Point Source Thermal Radiation Under Clouds in a Nonattenuating Medium," ECOM-5578, October 1975.

15. Norton, Colburn and Glenn Hoidale, "The Diurnal Variation of Mixing Height by Month over White Sands Missile Range, NM," ECOM-5579, November 1975.

16. Avara, Elton P., "On the Spectrum Analysis of Binary Data," ECOM-5580, November 1975.

17. Taylor, Fredrick J., Thomas H. Pries, and Chao-Huan Huang, "Optimal Wind Velocity Estimation," ECOM-5581, December 1975.

18. Avara, Elton P., "Some Effects of Autocorrelated and Cross-Correlated Noise on the Analysis of Variance," ECOM-5582, December 1975.

19. Gillespie, Patti S., R. L. Armstrong, and Kenneth O. White, "The Spectral Characteristics and Atmospheric CO_2 Absorption of the Ho^{+3}:YLF Laser at 2.05μm," ECOM-5583, December 1975.

20. Novlan, David J., "An Empirical Method of Forecasting Thunderstorms for the White Sands Missile Range," ECOM-5584, February 1976.

21. Avara, Elton P., "Randomization Effects in Hypothesis Testing with Autocorrelated Noise," ECOM-5585, February 1976.

22. Watkins, Wendell R., "Improvements in Long Path Absorption Cell Measurement," ECOM-5586, March 1976.

23. Thomas, Joe, George D. Alexander, and Marvin Dubbin, "SATTEL - An Army Dedicated Meteorological Telemetry System," ECOM-5587, March 1976.

24. Kennedy, Bruce W. and Delbert Bynum, "Army User Test Program for the RDT&E-XM-75 Meteorological Rocket," ECOM-5588, April 1976.

25. Barnett, Kenneth M., "A Description of the Artillery Meteorological Comparisons at White Sands Missile Range, October 1974 - December 1974 ('PASS'-Prototype Artillery [Meteorological] Subsystem)," ECOM-5589, April 1976.

26. Miller, Walter B., "Preliminary Analysis of Fall-of-Shot From Project 'PASS'," ECOM-5590, April 1976.

27. Avara, Elton P., "Error Analysis of Minimum Information and Smith's Direct Methods for Inverting the Radiative Transfer Equation," ECOM-5591, April 1976.

28. Yee, Young P., James D. Horn, and George Alexander, "Synoptic Thermal Wind Calculations from Radiosonde Observations Over the Southwestern United States," ECOM-5592, May 1976.

29. Duncan, Louis D. and Mary Ann Seagraves, "Applications of Empirical Corrections to NOAA-4 VTPR Observations," ECOM-5593, May 1976.

30. Miers, Bruce T. and Steve Weaver, "Application of Meteorological Satellite Data to Weather Sensitive Army Operations," ECOM-5594, May 1976.

31. Sharenow, Moses, "Redesign and Improvement of Balloon ML-566," ECOM-5595, June 1976.

32. Hansen, Frank V., "The Depth of the Surface Boundary Layer," ECOM-5596, June 1976.

33. Pinnick, R. G. and E. B. Stenmark, "Response Calculations for a Commercial Light-Scattering Aerosol Counter," ECOM-5597, July 1976.

DISTRIBUTION LIST

Commanding Officer
Picatinny Arsenal
ATTN: SARPA-TS-S, #59
Dover, NJ 07801

Commanding Officer
Harry Diamond Laboratory
ATTN: Library
2800 Powder Mill Road
Adelphi, MD 20783

Commander
US Army Electronics Command
ATTN: DRSEL-RD-D
Fort Monmouth, NJ 07703

Naval Surface Weapons Center
Code DT 21 (Ms. Greeley)
Dahlgren, VA 22448

Air Force Weapons Laboratory
ATTN: Technical Library (SUL)
Kirtland AFB, NM 87117

Director
US Army Engr Waterways Exper Sta
ATTN: Library Branch
Vicksburg, MS 39180

Commander
US Army Electronics Command
ATTN: DRSEL-CT-D
Fort Monmouth, NJ 07703

Meteorologist in Charge
Kwajalein Missile Range
PO Box 67
APO
San Francisco, CA 96555

Environmental Protection Agency
Meteorology Laboratory
Research Triangle Park, NC 27711

Chief, Technical Services Div
DCS/Aerospace Sciences
ATTN: AWS/DNTI
Scott AFB, IL 62225

Air Force Cambridge Rsch Labs
ATTN: LCH (A. S. Carten, Jr.)
Hanscom AFB
Bedford, MA 01731

Department of the Air Force
16WS/DO
Fort Monroe, VA 23651

Director
US Army Ballistic Research Lab
ATTN: DRXBR-AM
Aberdeen Proving Ground, MD 21005

Geophysics Division
Code 3250
Pacific Missile Test Center
Point Mugu, CA 93042

National Center for Atmos Res
NCAR Library
PO Box 3000
Boulder, CO 80303

William Peterson
Research Association
Utah State University, UNC 48
Logan, UT 84322

Commander
US Army Dugway Proving Ground
ATTN: MT-S
Dugway, UT · 84022

Head, Rsch and Development Div (ESA-131)
Meteorological Department
Naval Weapons Engineering Support Act
Washington, DC 20374

Commander
US Army Electronics Command
ATTN: DRCDE-R
5001 Eisenhower Avenue
Alexandria, VA 22304

Marine Corps Dev & Educ Cmd
Development Center
ATTN: Cmd, Control, & Comm Div (C^3)
Quantico, VA 22134

Commander
US Army Electronics Command
ATTN: DRSEL-WL-D1
Fort Monmouth, NJ 07703

Commander
US Army Missile Command
ATTN: DRSMI-RFGA, B. W. Fowler
Redstone Arsenal, AL 35809

Dir of Dev & Engr
Defense Systems Div
ATTN: SAREA-DE-DDR
H. Tannenbaum
Edgewood Arsenal, APG, MD 21010

Mr. William A. Main
USDA Forest Service
1407 S. Harrison Road
East Lansing, MI 48823

Naval Surface Weapons Center
Technical Library and Information
Services Division
White Oak, Silver Spring, MD 20910

Dr. A. D. Belmont
Research Division
PO Box 1249
Control Data Corp
Minneapolis, MN 55440

Dir, Elec Tech and Devices Lab
US Army Electronics Command
ATTN: DRSEL-TL-D, Bldg 2700
Fort Monmouth, NJ 07703

Director
Development Center MCDEC
ATTN: Firepower Division
Quantico, VA 22134

Commander
US Army Proving Ground
ATTN: Technical Library, Bldg 2100
Yuma, AZ 85364

US Army Liaison Office
MIT-Lincoln Lab, Library A-082
PO Box 73
Lexington, MA 02173

Library-R-51-Tech Reports
Environmental Research Labs
NOAA
Boulder, CO 80302

Head, Atmospheric Research Section
National Science Foundation
1800 G. Street, NW
Washington, DC 20550

Commander
US Army Missile Command
ATTN: DRSMI-RR
Redstone Arsenal, AL 35809

Commandant
US Army Field Artillery School
ATTN: Met Division
Fort Sill, OK 73503

Meteorology Laboratory
AFCRL/LY
Hanscom AFB
Bedford, MA 01731

Commander
US Army Engineer Topographic Lab
(STINFO CENTER)
Fort Belvoir, VA 22060

Commander
US Army Missile Command
ATTN: DRSMI-RRA, Bldg 7770
Redstone Arsenal, AL 35809

Air Force Avionics Lab
ATTN: AFAL/TSR
Wright-Patterson AFB, Ohio 45433

Commander
US Army Electronics Command
ATTN: DRSEL-VL-D
Fort Monmouth, NJ 07703

Commander
USAICS
ATTN: ATSI-CTD-MS
Fort Huachuca, AZ 85613

E&R Center
Bureau of Reclamation
ATTN: Bldg 67, Code 1210
Denver, CO 80225

HQDA (DAEN-RDM/Dr. De Percin)
Forrestal Bldg
Washington, DC 20314

Commander
Air Force Weapons Laboratory
ATTN: AFWL/WE
Kirtland AFB, NM 87117

Commander
US Army Satellite Comm Agc
ATTN: DRCPM-SC-3
Fort Monmouth, NJ 07703

Commander
US Army Electronics Command
ATTN: DRSEL-MS-TI
Fort Monmouth, NJ 07703

Commander
US Army Electronics Command
ATTN: DRSEL-GG-TD
Fort Monmouth, NJ 07703

Dr. Robert Durrenberger
Dir, The Lab of Climatology
Arizona State University
Tempe, AZ 85281

Commander
Headquarters, Fort Huachuca
ATTN: Tech Ref Div
Fort Huachuca, AZ 85613

Field Artillery Consultants
1112 Becontree Drive
ATTN: COL Buntyn
Lawton, OK 73501

Commander
US Army Nuclear Agency
ATTN: ATCA-NAW
Building 12
Fort Bliss, TX 79916

Director
Atmospheric Physics & Chem Lab
Code 31, NOAA
Department of Commerce
Boulder, CO 80302

Dr. John L. Walsh
Code 5503
Navy Research Lab
Washington, DC 20375

Commander
US Army Air Defense School
ATTN: C&S Dept, MSLSCI Div
Fort Bliss, TX 79916

Director National Security Agency
ATTN: TDL (C513)
Fort George G. Meade, MD 20755

USAF EPAC/CBT (Stop 825)
ATTN: Mr. Burgmann
Scott AFB, IL 62225

Armament Dev & Test Center
ADTC (DLOSL)
Eglin AFB, Florida 32542

Commander
US Army Ballistic Rsch Labs
ATTN: DRXBR-IB
Aberdeen Proving Ground, MD 21005

Director
Naval Research Laboratory
Code 2627
Washington, DC 20375

Commander
Naval Elect Sys Cmd HQ
Code 51014
Washington, DC 20360

The Library of Congress
ATTN: Exchange & Gift Div
Washington, DC 20540
2

CO, US Army Tropic Test Center
ATTN: STETC-MO-A (Tech Lib)
APO New York 09827

Commander
Naval Electronics Lab Center
ATTN: Library
San Diego, CA 92152

Office, Asst Sec Army (R&D)
ATTN: Dep for Science & Tech
Hq, Department of the Army
Washington, DC 20310

Director
US Army Ballistic Research Lab
ATTN: DRXBR-AM, Dr. F. E. Niles
Aberdeen Proving Ground, MD 21005

Commander
Frankford Arsenal
ATTN: Library, K2400, Bldg 51-2
Philadelphia, PA 19137

Director
US Army Ballistic Research Lab
ATTN: DRXBR-XA-LB
Bldg 305
Aberdeen Proving Ground, MD 21005

Dir, US Naval Research Lab
Code 5530
Washington, DC 20375

Commander
Office of Naval Research
Code 460-M
Arlington, VA 22217

Commander
Naval Weather Service Command
Washington Navy Yard
Bldg 200, Code 304
Washington, DC 20374

Technical Processes Br
D823
Room 806, Libraries Div NOAA
8060 13th St
Silver Spring, MD 20910

The Environmental Rsch Institute of MI
ATTN: IRIA Library
PO Box 618
Ann Arbor, MI 48107

Redstone Scientific Info Center
ATTN: Chief, Documents
US Army Missile Command
Redstone Arsenal, AL 35809

Commander
Edgewood Arsenal
ATTN: SAREA-TS-L
Aberdeen Proving Ground, MD 21010

Sylvania Elec Sys Western Div
ATTN: Technical Reports Library
PO Box 205
Mountain View, CA 94040

Commander
US Army Security Agency
ATTN: IARD-OS
Arlington Hall Station
Arlington, VA 22212
2

President
US Army Field Artillery Board
Fort Sill, OK 73503

Commandant
US Army Field Artillery School
ATTN: ATSF-TA-R
Fort Sill, OK 73503

CO, USA Foreign Sci & Tech Center
ATTN: DRXST-ISI
220 7th Street, NE
Charlottesville, VA 22901

Commander, Naval Ship Sys Cmd
Technical Library, Rm 3 S-08
National Center No. 3
Washington, DC 20360

Commandant
US Army Signal School
ATTN: ATSN-CD-MS
Fort Gordon, GA 30905

Rome Air Development Center
ATTN: Documents Library
TILD (Bette Smith)
Griffiss Air Force Base, NY 13441

HQ, ESD/DRI/S-22
Hanscom AFB
MA 01731

Commander
Frankford Arsenal
ATTN: J. Helfrich PDSP 65-1
Philadelphia, PA 19137

Director
Defense Nuclear Agency
ATTN: Tech Library
Washington, DC 20305

Department of the Air Force
5WW/DOX
Langley AFB, VA 23665

Commander
US Army Missile Command
ATTN: DRSMI-RER (Mr. Haraway)
Redstone Arsenal, AL 35809

CPT Hugh Albers, Exec Sec
Interdept Committee on Atmos Sci
Fed Council for Sci & Tech
National Sci Foundation
Washington, DC 20550

US Army Research Office
ATTN: DRXRO-IP
PO Box 12211
Research Triangle Park, NC 27709

Commander
US Army Training & Doctrine Cmd
ATTN: ATCD-SC
Fort Monroe, VA 23651

Mil Assistant for Environmental Sciences
OAD (E & LS), 3D129
The Pentagon
Washington, DC 20301

Commander
Eustis Directorate
US Army Air Mobility R&D Lab
ATTN: Technical Library
Fort Eustis, VA 23604

National Weather Service
National Meteorological Center
World Weather Bldg - 5200 Auth Rd
ATTN: Mr. Quiroz
Washington, DC 20233

Commander
US Army Materiel Command
ATTN: DRCRD-SS (Mr. Andrew)
Alexandria, VA 22304

Commander
Frankford Arsenal
ATTN: SARFA-FCD-O, Bldg 201-2
Bridge & Tarcony Sts
Philadelphia, PA 19137

Inge Dirmhirn, Professor
Utah State University, UMC 48
Logan, UT 84322

Chief, Aerospace Environ Div
Code ES41
NASA
Marshall Space Flight Center, AL 35802

Dr. Frank D. Eaton
PO Box 3038
University Station
Laramie, Wyoming 82071

Commander
US Army Arctic Test Center
ATTN: STEAC-OP-PL
APO Seattle 98733

Commander
US Army Electronics Command
ATTN: DRSEL-GS-H (Stevenson)
Fort Monmouth, NJ 07703

Commander
USACACDA
ATTN: ATCA-CCC-W
Fort Leavenworth, KS 66027

Commander
US Army Test & Eval Cmd
ATTN: DRSTE-FA
Aberdeen Proving Ground, MD 21005

Air Force Cambridge Rsch Labs
ATTN: LKI
L. G. Hanscom Field
Bedford, MA 01730

Director, Systems R&D Service
Federal Aviation Administration
ATTN: ARD-54
2100 Second Street, SW
Washington, DC 20590

USAFETAC/CB (Stop 825)
Scott AFB
IL 62225

Director
USAE Waterways Experiment Station
ATTN: Library
PO Box 631
Vicksburg, MS 39180

Defense Documentation Center
ATTN: DDC-TCA
Cameron Station (BLDG 5)
Alexandria, Virginia 22314
12

Commander
US Army Electronics Command
ATTN: DRSEL-CT-S
Fort Monmouth, NJ 07703

Commander
Holloman Air Force Base
6585 TG/WE
Holloman AFB, NM 88330

Commandant
USAFAS
ATTN: ATSF-CD-MT (Mr. Farmer)
Fort Sill, OK 73503
2

Commandant
USAFAS
ATTN: ATSF-CD-C (Mr. Shelton)
Fort Sill, OK 73503
2

Commander
US Army Electronics Command
ATTN: DRSEL-CT-S (Dr. Swingle)
Fort Monmouth, NJ 07703
3